UNNS Substrate Research Program | Working Manuscript

Charge Boundary Routing:

Fractional Coordinates, Composite Closure, and Route-Preserving Transitions

Instruments: STRUC-PERC-I v2.5.0 · STRUC-I v1.0.4

Corpus: 40 charge-boundary objects · 5 bridge corpora · 10 pairwise same-charge control pairs · 38 allowed transitions · 48 Phase 3C boundary tests

Data: PDG RPP 2026 Summary Tables

Status: Charge Boundary Routing I — Phases 1–3C complete · Date: 2026

Abstract

Electric charge is ordinarily represented as a scalar conserved quantity, yet equal charge values may occur in structurally different carriers: a positron, a proton, and a W^+ boson all carry $Q/e = +1$ while occupying fundamentally different physical roles. This manuscript introduces **Charge Boundary Routing**, a framework within the UNNS (Unbounded Nested Number Sequences) Substrate for representing electric charge not only as a scalar value Q but as a routed boundary structure involving external free-closure states, confined fractional coordinates, composite closure, boundary absences, and route-preserving transitions.

A four-layer charge corpus of 40 PDG-sourced objects separates **Layer A** (14 external/free closure states), **Layer B** (12 confined fractional quark coordinates), **Layer C** (10 composite hadron closures), and **Layer D** (4 boundary absences or constraints). Using STRUC-PERC-I graph connectivity and STRUC-I perturbative admissibility analysis across six phases, we establish the central quantitative distinction: scalar charge-value encodings produce Hard Fragmentation at layer interfaces where route and closure encodings reach Full Percolation. A pairwise same-charge control over $Q/e = +1$ objects demonstrates that equal charge does not imply equal structural route: the `structural_route_pair_code` encoding reaches Geometric Persistence/Stable Structure with $\langle A_\kappa \rangle = 1.000$, while trivial same-charge encodings remain Transitional. Seed and expanded transition corpora (7 and 38 allowed transitions respectively) show that allowed transitions preserve route and closure transition geometry beyond total charge balance alone. In the expanded corpus, `route_transition_code` and `closure_transition_code` advance to Geometric Persistence/Boundary-Stabilized with $\langle A_\kappa \rangle \approx 0.985$ and 0.984 respectively. A further Phase 3C contrast corpus of 48 allowed, forbidden, constrained, free-fractional, and route-incoherent transition candidates shows that the mixed corpus remains globally connected under STRUC-PERC-I, but loses perturbative route-transition admissibility under STRUC-I. In particular, `route_transition_code` falls from Geometric Persistence / Boundary-Stabilized ($\langle A_\kappa \rangle = 0.985$) to Structural Boundary / Transitional Structure ($\langle A_\kappa \rangle = 0.859$) in Phase 3C, while `closure_transition_code` remains Boundary-Stabilized. Together, these results support the interpretation that charge conservation is the visible projection of a deeper boundary-route preservation structure, and that charge balance is necessary but not sufficient for transition admissibility.

Contents

1 Introduction

Electric charge is one of the most precisely conserved quantities in nature. The conservation law $\sum Q_{\text{initial}} = \sum Q_{\text{final}}$ holds to extraordinary precision across every recorded interaction. Charge is quantized in observed free states and is assigned as a scalar property to every particle in the Standard Model.

Yet this scalar assignment conceals a structural heterogeneity that standard bookkeeping does not address. Consider five objects that all carry $Q/e = +1$:

- the positron e^+: an elementary external lepton closure;
- the proton p: a composite baryon formed from three quarks (uud);
- the positive pion π^+: a composite meson formed from $u\bar{d}$;
- the positive kaon K^+: a composite strange meson ($u\bar{s}$);
- the W^+ boson: an external gauge-sector closure.

These five objects are indistinguishable from the perspective of external charge bookkeeping. They all enter conservation equations identically. But they differ in confinement status, internal composition, quark content, generation assignment, and the physical mechanism by which they carry their charge. The scalar Q does not distinguish them.

This manuscript addresses the question: *should charge be represented by route and closure coordinates in addition to scalar value?*

We answer affirmatively through a structured empirical program within the UNNS Substrate framework. The central thesis is:

Thesis. *Charge Boundary Routing treats Q as a projection of a deeper structural route involving closure, confinement, composition, and boundary status. Charge value is a projection; structural route is a separate coordinate.*

The program proceeds in six phases: static boundary classification (Phase 1), bridge geometry between layers (Phase 2), a same-charge route control (Phase 2C-P), seed transition dynamics (Phase 3), expanded transition robustness (Phase 3B), and forbidden / constrained transition boundary testing (Phase 3C). Together these phases establish a coherent charge-boundary framework that is anchored in PDG-sourced particle data and evaluated through two independent chamber instruments.

Organization. Section 2 situates the work relative to standard charge physics. Section 3 defines the UNNS charge-routing ontology. Section 4 describes corpus construction. Section 5 explains the chamber instruments. Sections 6–11 present results. Section 12 integrates the findings. Section 13 positions the work relative to existing theory. Sections 14–16 address limitations, next work, and conclusions.

Contributions. This manuscript contributes:

(i) a four-layer charge-boundary taxonomy separating external closure states, confined fractional coordinates, composite closures, and boundary absences;
(ii) bridge tests demonstrating that charge-value topology and route/closure topology are not equivalent across the tested layer interfaces;

(iii) a pairwise same-charge control showing that equal $Q/e = +1$ does not imply equal structural route;
(iv) seed and expanded transition analyses showing that allowed transitions preserve route and closure geometry beyond total charge balance alone; and
(v) a Phase 3C forbidden / constrained contrast test showing that mixed allowed-forbidden transition space remains percolatively connected but loses route-transition admissibility.

2 Background and Motivation

2.1 Standard scalar charge bookkeeping

In the Standard Model, electric charge Q is a conserved additive quantum number associated with the U(1) gauge symmetry of electromagnetism. Every field is assigned a definite charge eigenvalue, and conservation requires that the total charge of any closed system does not change. This framework is extraordinarily successful. Charge neutrality tests, for example, constrain the proton–electron charge mismatch to $|q_p + q_e|/e < 10^{-21}$ [1], and no charge-conservation–violating decay has been confirmed.

The scalar assignment is operationally complete for bookkeeping purposes. However, it is structurally silent on the question of *how* a given charge value is embodied.

2.2 Fractional quark charges

Quarks carry electric charges of $\pm 1/3\, e$ and $\pm 2/3\, e$, values that are not observed for free external states. Despite carrying well-defined fractional charges, isolated quarks have not been experimentally confirmed. Every search for free quarks since 1977 has returned negative results [1].

This creates a structural puzzle that scalar bookkeeping does not resolve: fractional charges exist as valid internal quantities but do not appear as free external objects. The standard interpretation is color confinement within quantum chromodynamics, but this leaves the charge-routing question implicit: what prevents a fractional charge from becoming a free external closure?

2.3 Composite charge closure in hadrons

In the quark model, the electric charge of a hadron is computed as the arithmetic sum of its constituent quark charges. For the proton (uud):

$$Q_p = \tfrac{2}{3} + \tfrac{2}{3} - \tfrac{1}{3} = +1.$$

For the neutron (udd):

$$Q_n = \tfrac{2}{3} - \tfrac{1}{3} - \tfrac{1}{3} = 0.$$

This summation is arithmetically correct, but it characterizes a composite state only as a charge total. It does not address the fact that the fractional internal coordinates are physically confined and that the integer or neutral result appears only at the external, observable boundary of the hadron.

We will argue that this process is more accurately characterized as *closure*: internal fractional route coordinates close into an external integer or neutral charge state.

2.4 Non-observation of free fractional charge

The non-observation of free fractional charge is not merely an absence of data. It is a structural boundary condition: the charge-routing system refuses to externalize fractional values. In the UNNS framework, this is naturally represented as a *boundary object*—a member of the charge corpus that marks where externalization fails.

Standard physics represents this as confinement. The UNNS framework represents it as a terminal obstruction in the charge-routing system.

2.5 Charge-conserving transitions

Allowed particle transitions, such as neutron beta decay ($n \to p + e^- + \bar{\nu}_e$), are constrained by charge conservation $Q_i = Q_f$. These selection rules are well-established and have been tested to high precision.

However, charge conservation alone does not distinguish allowed from forbidden transitions at the structural level. One can construct mock transitions that conserve charge but violate other selection rules. The question therefore arises: do allowed transitions carry a deeper structural signature beyond $Q_i = Q_f$?

2.6 Why scalar Q alone is structurally incomplete

The five observations above suggest a structural gap:

1. Equal Q can occur in structurally different carriers.
2. Fractional Q is internally valid but not externally free.
3. Composite Q is formed by a confinement-and-closure operation.
4. Absent external Q states are structured boundary conditions.
5. Allowed transitions may carry route/closure geometry beyond $Q_i = Q_f$.

This manuscript addresses all five gaps through the Charge Boundary Routing framework.

3 UNNS Charge-Boundary Framework

3.1 Core ontology

The UNNS (Unbounded Nested Number Sequences) Substrate is a formal framework for representing structured physical systems through admissibility geometry, realizability space, and percolative structural analysis. In the charge-boundary specialization, the framework assigns to each charge-bearing object a *route coordinate tuple* in addition to its scalar charge value.

Definition 3.1 (Charge Value)**.** The charge value $Q \in \mathbb{Q}$ is the scalar electric charge of an object expressed in units of e. In the UNNS representation, Q is a projection of the full route structure onto the observable charge axis.

Definition 3.2 (Route Coordinate)**.** A route coordinate $r \in \mathcal{R}$ is a categorical structural attribute that specifies how a charge-bearing object acquires and expresses its charge. Route coordinates include the closure class, the confinement state, the composition status, and the boundary condition.

Definition 3.3 (Closure Class)**.** The closure class $\mathcal{C}(L)$ of a charge-bearing object L specifies the terminal form of its external charge expression. The nine closure classes in the Phase 1

corpus are:

`FREE_INTEGER_CLOSURE` • `FREE_NEUTRAL_CLOSURE` • `INTERNAL_FRACTIONAL_CO-ORDINATE` • `COMPOSITE_INTEGER_CLOSURE` • `COMPOSITE_NEUTRAL_CLOSURE` • `TERMINAL_FREE_FRACTIONAL` • `UNRESOLVED_DUAL_BOUNDARY` • `CONSTRAINED_CHARGE_VIOLATION_BOUNDARY` • `EXTERNAL_NEUTRALITY_CONSTRAINT`

Definition 3.4 (Structural Route)**.** The structural route of an object L is the full tuple (Q, layer, route class, closure class, boundary state, composition state). The charge value Q is the scalar projection; the remaining coordinates specify the admissibility route.

3.2 Four-layer taxonomy

The charge-routing ontology organizes charge-bearing objects into four layers (Figure 1):

Definition 3.5 (Layer A — External/Free Closure States)**. Layer A** consists of charge-bearing objects that appear as externally observable, freely propagating closure states. Their charge expression is direct and external: no compositional step is required between their internal structure and their observable charge value. Examples include charged leptons, neutrinos, photons, $\mathrm{W}^{\pm}$, Z^0, and the Higgs boson.

Definition 3.6 (Layer B — Confined Fractional Coordinates)**. Layer B** consists of quark and antiquark charge coordinates. These objects carry fractional electric charges ($\pm 1/3$, $\pm 2/3$) that are locally valid as internal route coordinates but are not externally free. Fractional charge is represented as a confined internal route coordinate, not as a failed external charge.

Definition 3.7 (Layer C — Composite Closures)**. Layer C** consists of hadrons (baryons and mesons) in which internal fractional coordinates close into integer or neutral external charge states. The closure operation is not merely arithmetic summation; it is the structural formation of an admissible composite route. Composite charge is closure, not merely summation.

Definition 3.8 (Layer D — Boundary Absences and Constraints)**. Layer D** consists of empirically constrained absence objects: free quark searches (negative result), magnetic monopole searches (negative result), charge-violation test modes (upper-bounded), and external neutrality constraints. Boundary absence is structural, not simply missing data. **Layer D** objects mark where the charge-routing system refuses to externalize certain charge configurations.

3.3 Key structural principles

Principle 3.9 (Charge Value is a Projection)**.** Observable charge value Q is the projection of a multi-coordinate structural route onto the charge axis. The route coordinate carries information not available in Q alone.

Principle 3.10 (Route-Preserving Transition)**.** An allowed charge-conserving transition is not only $Q_i = Q_f$. It is a structural transformation that carries route and closure coordinates from an initial configuration to a final configuration while preserving admissibility.

Principle 3.11 (Boundary-Route Invariant)**.** Charge conservation is the visible projection; boundary-route preservation is the structural invariant.

3.4 UNNS charge-routing tuple representation

The representational upgrade proposed by this framework replaces the scalar representation

$$\text{charge object} \longleftrightarrow Q$$

with the route tuple

$$\text{charge object} \longleftrightarrow (Q,\ \ell,\ r,\ \mathcal{C},\ b,\ s_{\text{comp}})$$

where ℓ is the layer assignment, r is the route class, $\mathcal{C}$ is the closure class, b is the boundary state, and s_{comp} is the composition status.

4 Data and Corpus Construction

4.1 Phase 1 object corpus

The Phase 1 corpus contains 40 objects assigned to Layers A–D and encoded with UNNS route and closure attributes (Table 1). All objects are PDG-sourced or PDG-aligned from RPP 2026 summary tables [1].

Layer A (14 objects): charged leptons ($e^{\pm}$, $\mu^{\pm}$, $\tau^{\pm}$), three neutrino flavors (ν_e, ν_μ, ν_τ), photon (γ), $W^{\pm}$, Z^0, and Higgs (H). These are the free external closure states: 8 carry `FREE_INTEGER_CLOSURE` and 6 carry `FREE_NEUTRAL_CLOSURE`. All are classified as `EXTERNAL_CLOSURE` in the route class.

Layer B (12 objects): six quarks (u, d, s, c, b, t) and their six antiquarks. All 12 carry `INTERNAL_FRACTIONAL_COORDINATE` closure class and `CONFINED_ROUTE` route class. Quark charges span $\{+2/3, -1/3\}$.

Layer C (10 objects): proton p ($uud \to +1$), neutron n ($udd \to 0$), Delta baryon Δ^{++} ($uuu \to +2$), Omega baryon Ω^- ($sss \to -1$), charged pions $\pi^{\pm}$ ($u\bar{d} \to +1$ and $\bar{u}d \to -1$), neutral pion π^0 (composite neutral meson; transition source in Phase 3 as $\pi^0 \to \gamma\gamma$, not a primitive carrier), $K^{\pm}$ and K^0. These carry 7 `COMPOSITE_INTEGER_CLOSURE` and 3 `COMPOSITE_NEUTRAL_CLOSURE`.

Layer D (4 objects): free quark absence (not confirmed externally; `TERMINAL_FREE_FRACTIONAL`); magnetic monopole (not confirmed; `UNRESOLVED_DUAL_BOUNDARY`); neutron charge-violating mode $n \to p\nu_e\bar{\nu}_e$ (constrained upper bound; `CONSTRAINED_CHARGE_VIOLATION_BOUNDARY`); proton–electron charge mismatch bound $|q_p + q_e|/e < 10^{-21}$ (`EXTERNAL_NEUTRALITY_CONSTRAINT`).

Layer D objects are not failed rows. They are boundary conditions of the charge-routing system. When submitted to STRUC-I, Layer D ladder files were rejected as non-numeric, since their rows encode boundary-condition descriptors and constrained values rather than perturbable numeric states. This rejection is treated as a diagnostic consequence of how Layer D was encoded: it supports, but does not by itself prove, the interpretation of these objects as structural limit markers rather than ordinary runnable ladders.

4.2 Phase 2 bridge corpora

Five bridge corpora were constructed by combining adjacent or spanning layers:

- **AB**: external/free closure states ∪ confined fractional coordinates (26 objects);
- **BC**: confined fractional coordinates ∪ composite closures (22 objects);

- **CD**: composite closures ∪ boundary absences (14 objects);
- **ABC**: all three internal-plus-external layers (36 objects);
- **BCD**: fractional, composite, and boundary layers (26 objects).

Each bridge corpus was encoded with the same six ladder attributes as Phase 1 (absolute charge, signed charge, boundary route coordinate, closure class code, closure state code, route class code) and submitted to the chambers independently.

4.3 Phase 2C-P same-charge route control

Five objects all carrying $Q/e = +1$ were selected as control objects: e^+ (external lepton), p (composite baryon), π^+ (composite meson), K^+ (composite strange meson), and W^+ (external gauge boson). These five objects were expanded into all $\binom{5}{2} = 10$ unordered pairs, yielding 10 pair rows encoding structural differences between same-charge objects. The charge difference $\Delta Q = 0$ for every pair by construction.

The control question is: *when $\Delta Q = 0$ for every pair, do structural route differences remain nonzero?*

4.4 Phase 3 seed transition corpus

Seven canonical allowed transitions were selected as seed cases (Table 5):

T1. neutron beta decay: $n \to p + e^- + \bar{\nu}_e$

T2. positive pion muonic decay: $\pi^+ \to \mu^+ + \nu_\mu$

T3. negative muon decay: $\mu^- \to e^- + \bar{\nu}_e + \nu_\mu$

T4. W^- leptonic decay: $W^- \to e^- + \bar{\nu}_e$

T5. W^+ leptonic decay: $W^+ \to e^+ + \nu_e$

T6. neutral pion two-photon decay: $\pi^0 \to \gamma + \gamma$

T7. positive kaon muonic decay: $\mathrm{K}^+ \to \mu^+ + \nu_\mu$

All seven conserve total charge (verified: $\Delta Q = 0$ for all transitions). Each transition is encoded with initial and final total charge, route transition code, closure transition code, layer transition code, transition class, and particle count deltas.

4.5 Phase 3B expanded transition corpus

Starting from the 7 seed transitions, 31 expansion transitions were added, bringing the corpus to 38 allowed transitions across 8 decay families: baryon decay (8), charged meson decay (6), W/Z-mediated channel (6), neutral meson decay (5), seed continuity (7), baryon resonance decay (2), neutral or charged vector meson decay (2), and radiative decay (2).

All 38 transitions conserve charge ($\Delta Q = 0$; maximum absolute charge balance error = 0.000).

4.6 Phase 3C forbidden and constrained transition corpus

Phase 3C constructs a 48-row contrast corpus designed to test whether forbidden, constrained, free-fractional, and route-incoherent transitions occupy different route / closure admissibility regimes from the allowed Phase 3B corpus. The corpus contains six groups: (A) 12 allowed controls selected from the Phase 3B interior; (B) 8 charge-violating mock

transitions; (C) 8 free-fractional externalization attempts; (D) 8 selection-rule violating comparison channels; (E) 8 route-incoherent charge-conserving mocks; and (F) 4 constrained or upper-bounded boundary cases. Forty rows are charge-balanced and eight rows deliberately violate charge balance. This design separates direct charge-balance failure from the deeper UNNS test: whether charge-conserving but route-incoherent transitions fail route / closure admissibility.

Canonical corpus: `phase3C_forbidden_constrained_transition_corpus.csv` (48 rows, 71 columns, 43 ladders).

Derived summary: `phase3C_forbidden_constrained_transition_summary.json`. Chamber comparison report: `PHASE3C_FORBIDDEN_BOUNDARY_chamber_comparison_report.txt`.

Source statement. All Phase 1 object data are PDG-sourced or PDG-aligned from the following RPP 2026 summary tables [1]: Leptons, Gauge and Higgs Bosons, Quarks, Mesons, Baryons, and Searches. Phase 3 and Phase 3B transition data are drawn from established branching ratios in the same source.

5 Methods

5.1 Ladder encoding

Each corpus is encoded as a set of one-column ladder files, one per structural attribute (encoding). Each ladder file contains a single column of numeric values, one per corpus object or transition. Categorical attributes (route class, closure class, transition type) are encoded as integer codes. Continuous attributes (absolute charge, signed charge) are encoded as floating-point values.

Two ladder variants are produced for each encoding: a full provenance ladder (including row identifiers, metadata, and values) and a one-column chamber input ladder (values only). The one-column variant is submitted to the chambers.

Categorical codes are used only as reproducible structural labels; their numerical ordering is not interpreted as a physical magnitude unless the encoded attribute is intrinsically numeric (as in absolute or signed charge values).

Phase 3C uses the same ladder and chamber protocol as Phases 3 and 3B, but introduces explicit contrast encodings: `route_charge_consistency_code`, `closure_charge_consistency_code`, `allowed_vs_forbidden_code`, `boundary_pressure_index`, `boundary_response_code`, `transition_status_code`, and diagnostic flags for charge violation, free-fractional externalization, selection violation, route incoherence, constraint status, and forbiddenness. As in the earlier phases, categorical codes are interpreted only as reproducible structural labels.

5.2 STRUC-PERC-I v2.5.0

STRUC-PERC-I tests whether a one-column numeric ladder forms a connected percolation structure across a range of coupling parameter $\kappa \in [0, \kappa_{\max}]$.

The instrument constructs a graph in which nodes are ladder rows and edges are added between rows whose values differ by at most κ-scaled tolerance. As κ increases, the graph density grows. The instrument records:

- **Giant ratio** GR: fraction of nodes in the largest connected component at $\kappa_{\max}$.
- **Connectivity threshold** κ_{conn}: the κ value at which the giant component first spans the whole ladder.
- **Isolated fraction**: fraction of nodes never joining the giant component.

Verdicts:

- FULL_PERCOLATION: GR $= 1.000$, isolated $= 0$. The ladder is globally connected.
- HARD_FRAGMENTATION: GR < 1.000 or isolated > 0. The ladder contains permanently disconnected components.

5.3 STRUC-I v1.0.4

STRUC-I tests whether a ladder remains admissible under perturbation according to the admissibility inequality

$$\text{inv}(P_\varepsilon;\, L) \;\leq\; \nu(V_\varepsilon(L))\,, \tag{1}$$

where P_ε is a family of perturbation operators of scale ε, L is the ladder, $\text{inv}(\cdot)$ measures the perturbation-invariant fraction, and $\nu(V_\varepsilon(L))$ is the admissibility volume of the ε-neighborhood.

The primary output is the admissibility coefficient $A_\kappa \in [0, 1]$, evaluated at each κ step. Reported statistics:

- $\langle A_\kappa \rangle$: mean admissibility across all κ steps;
- $\min A_\kappa$: minimum admissibility (worst-case perturbation response).

Regime assignments:

- **Geometric Persistence** ($\langle A_\kappa \rangle \gtrsim 0.93$): the ladder retains coherent admissibility geometry under perturbation.
- **Structural Boundary** ($\langle A_\kappa \rangle \lesssim 0.93$): the ladder sits at or below the admissibility boundary.

State assignments within Geometric Persistence:

- STABLE STRUCTURE: $\langle A_\kappa \rangle = 1.000$, $\min A_\kappa = 1.000$.
- BOUNDARY-STABILIZED: $\langle A_\kappa \rangle \gtrsim 0.975$.
- WEAK PERSISTENCE: $0.93 \lesssim \langle A_\kappa \rangle < 0.975$.

State assignments within Structural Boundary:

- TRANSITIONAL STRUCTURE: $\langle A_\kappa \rangle < 0.93$.

6 Phase 1 Results: Boundary Classification

6.1 ABCD combined ladder

The 40-object ABCD combined ladder was encoded with six attributes and submitted to both chambers (results in Section 7, which addresses the cross-layer structure directly).

6.2 Layer-resolved chamber behavior

Layer A. When tested as an isolated set, signed charge is the only encoding reaching FULL_PERCOLATION under STRUC-PERC-I, with $\langle A_\kappa \rangle$ in the Weak Persistence range under

STRUC-I. All other encodings fragment within Layer A alone. Interpretation: Layer A is signed-charge coherent but route-taxonomy sparse. It acts as the external charge baseline of the routing system, not the whole system.

Layer B. All six encodings of Layer B reach FULL_PERCOLATION under STRUC-PERC-I. The absolute charge encoding achieves the highest STRUC-I score ($\langle A_\kappa \rangle = 0.925$, $\min A_\kappa = 0.904$), reflecting the regularity of the fractional charge set $\{\pm 1/3, \pm 2/3\}$. However, all encodings remain STRUCTURAL BOUNDARY/TRANSITIONAL STRUCTURE under STRUC-I, consistent with Layer B's role as an internal coordinate system rather than an external closure layer.

Layer C. Composite closure objects show partial percolation in charge-value encodings and reach FULL_PERCOLATION in route/closure encodings. The composite-closure structure organizes the layer and supports the interpretation that Layer C is route-connected internally.

Layer D. Layer D cannot be submitted as an ordinary numeric ladder. The STRUC-I chamber rejected all Layer D files as non-numeric, confirming that boundary-absence objects do not form a perturbable admissibility ladder. Layer D serves as a limit stratum—the boundary of the routing system—not as a runnable encoding corpus.

Finding 6.1. Charge-bearing objects are not one homogeneous charge class. The corpus separates naturally into four structurally distinct regimes: external free closure states, confined fractional coordinates, composite closures, and boundary absences. Layer D objects are boundary conditions of the charge-routing system, not failed data rows.

7 Phase 2 Results: Bridge Geometry

7.1 ABCD combined percolation and admissibility

The ABCD combined corpus (all 40 objects) was tested first. Table 3 presents the full bridge outcome summary.

Under STRUC-PERC-I, the six ABCD combined encodings split cleanly: absolute charge and signed charge both reach HARD_FRAGMENTATION (GR = 0.750 and 0.857 respectively); boundary route coordinate, closure class code, closure state code, and route class code all reach FULL_PERCOLATION. The same 40-object corpus produces opposite percolation verdicts depending on whether the encoding is charge-value or route/closure.

Under STRUC-I: the route class code encoding achieves the highest admissibility ($\langle A_\kappa \rangle = 0.919$), while signed charge achieves the lowest ($\langle A_\kappa \rangle = 0.657$). All six encodings remain STRUCTURAL BOUNDARY/TRANSITIONAL STRUCTURE, which is structurally correct for a corpus spanning four fundamentally different charge regimes.

7.2 Bridge-by-bridge outcomes

AB bridge (external ↔ fractional). Absolute charge and signed charge both fragment (HARD_FRAGMENTATION). Boundary route, closure class, closure state, and route class all reach FULL_PERCOLATION. Interpretation: the AB interface fragments in charge-value space but percolates in route/closure space. This is the first topological evidence that charge-value topology and charge-route topology are not equivalent.

BC bridge (fractional ↔ composite). Absolute charge reaches FULL_PERCOLATION ($\kappa_{\text{conn}} = 1.0$), reflecting the shared magnitude scale between quark charges and composite

closure results. Signed charge fragments (HARD_FRAGMENTATION, GR = 0.857), reflecting the sign incompatibility between fractional and composite objects in the combined space. Route, closure, and state encodings all reach FULL_PERCOLATION. Interpretation: BC is route-connected but admissibility-transitional. The fractional-to-composite bridge is the central route-formation step of the charge-routing system.

CD bridge (composite ↔ boundary absence). All four testable encodings reach HARD_FRAGMENTATION (GR ranging from 0.833 to 0.900). Interpretation: Layer D terminates the charge route. The boundary absence layer is not a smooth continuation of the composite closure layer; it marks a topological endpoint.

ABC bridge (external/fractional/composite). Absolute charge reaches FULL_PERCOLATION ($\kappa_{\text{conn}} = 1.0$); route class, closure class, and closure state all reach FULL_PERCOLATION. Signed charge and boundary route coordinate fragment. Interpretation: the composite layer partially mediates the external-to-fractional interface, restoring percolation in some channels while admissibility pressure remains.

BCD bridge (fractional/composite/boundary). All four testable encodings return HARD_FRAGMENTATION once Layer D is appended. Interpretation: the boundary absence layer acts as a terminal boundary condition at every interface it touches.

Finding 7.1. Charge-value topology is not equivalent to charge-route topology. Bare charge-value encodings can fragment while route and closure encodings percolate at the same interface. Boundary absence terminates the route; it does not extend it.

8 Phase 2C-P Results: Same-Charge Route Control

8.1 Control design

The Phase 2C-P control isolates the route-separation question from the charge question entirely. By fixing $Q/e = +1$ for every object and $\Delta Q = 0$ for every pair, any persistent signal in structural encodings cannot be attributed to charge variation. It must reflect genuine route differences.

The 10 pairs span three pair classes: 6 cross-layer same-charge pairs (e.g., e^+ and p), 3 same-layer different-category pairs (e.g., p and π^+), and 1 same-category different-subtype pair (π^+ and K^+).

8.2 STRUC-PERC-I result

All 27 tested pairwise encodings reach FULL_PERCOLATION (0 HARD_FRAGMENTATION). The control corpus is globally connected across every tested coordinate.

8.3 STRUC-I result

Table 4 presents the key STRUC-I outcomes. The most important result is:

Encoding	Regime/State	$\langle A_\kappa \rangle$
`structural_route_pair_code`	Geometric Persistence/Stable Structure	1.000
`sub_category_pair_code`	Geometric Persistence/Stable Structure	1.000
`category_pair_code`	Geometric Persistence/Weak Persistence	1.000
`charge_difference`	Structural Boundary/Transitional Structure	0.863
`same_charge_pair`	Structural Boundary/Transitional Structure	0.860

`structural_route_pair_code` and `sub_category_pair_code` reach Geometric Persistence/Stable Structure with $\langle A_\kappa \rangle = \min A_\kappa = 1.000$. These are the highest STRUC-I scores achievable.

Crucially, `charge_difference` and `same_charge_pair`—the trivial control encodings whose values are fixed (0 and 1 respectively for all pairs)—remain Structural Boundary/ Transitional Structure. The chamber did not reward charge equality; it detected route structure independently of charge equality.

The broader picture confirms route separation across all type-difference encodings: `baryon_difference`, `lepton_difference`, `hadron_difference`, `fermion_difference`, etc., all reach Geometric Persistence/Weak Persistence with $\langle A_\kappa \rangle \approx 0.940$–$0.943$.

Finding 8.1. Same $Q/e = +1$ does not imply same structural route. With charge equality fixed by construction, structural route and sub-category encodings reach Stable Structure ($A_\kappa = 1.000$) while trivial same-charge encodings remain Transitional. The persistent signal is route separation, not charge detection.

9 Phase 3 Results: Seed Transition Dynamics

9.1 From static objects to allowed transformations

Phase 3 moves from the static charge corpus to charge-conserving transitions. This is the dynamic version of the boundary-routing question: do allowed transitions preserve route and closure structure, or do they merely preserve the scalar sum $Q_i = Q_f$?

9.2 Seed corpus results

STRUC-PERC-I. 9 of 10 tested encodings reach FULL_PERCOLATION. The single HARD_FRAGMENTATION outcome is `charged_multiplicity_delta` (GR = 0.857, tail dominance = 0.997). This fragmentation is diagnostically meaningful: allowed transitions are not organized by how many charged objects appear or disappear. The transition system is not a "charged object count machine."

STRUC-I. The strongest encodings are:

- `route_transition_code`: Geometric Persistence/Weak Persistence, $\langle A_\kappa \rangle = 0.999925$
- `closure_transition_code`: Geometric Persistence/Weak Persistence, $\langle A_\kappa \rangle = 0.999925$
- `transition_class_code`: Geometric Persistence/Weak Persistence, $\langle A_\kappa \rangle = 0.999888$
- `initial_total_charge`: Geometric Persistence/Weak Persistence, $\langle A_\kappa \rangle =$

0.9575

- `final_total_charge`: Geometric Persistence/Weak Persistence, $\langle A_\kappa \rangle = 0.9565$

Count and multiplicity coordinates (`neutral_multiplicity_delta`, `externalization_delta`, `composite_count_delta`) remain Structural Boundary/ Transitional Structure, confirming that the persistent geometry does not concentrate in raw particle counts but in the route and closure transition structure.

Finding 9.1. Allowed transitions become weakly persistent in route-transition, closure-transition, and transition-class coordinates. Charge conservation is visible in total-charge encodings; boundary-route preservation is the stronger structural signal. The `charged_multiplicity_delta` fragmentation shows that transitions are not organized by charged-object count change.

10 Phase 3B Results: Expanded Transition Robustness

10.1 Robustness question

The Phase 3 seed result was obtained from 7 transitions. A critic could argue that 7 transitions are too few to support a general claim about route preservation. Phase 3B addresses this by expanding to 38 transitions across 8 decay families and asking whether the seed result survives.

10.2 STRUC-PERC-I result

21 of 21 tested encodings reach full_percolation (0 hard_fragmentation). This is stronger than the seed result. Notably, `charged_multiplicity_delta`—which fragmented in the 7-transition seed—reaches full_percolation in Phase 3B. The seed fragmentation was a small-corpus sensitivity, not a structural property of the allowed-transition system.

10.3 STRUC-I result

The key Phase 3B advancement is that route and closure transition encodings move from Weak Persistence (seed) to Boundary-Stabilized (expanded):

Encoding	Regime/State	$\langle A_\kappa \rangle$
`route_transition_code`	Geometric Persistence/Boundary-Stabilized	0.9851
`closure_transition_code`	Geometric Persistence/Boundary-Stabilized	0.9839
`category_transition_code`	Geometric Persistence/Boundary-Stabilized	0.9776
`transition_class_code`	Geometric Persistence/Boundary-Stabilized	0.9775
`transition_family_code`	Geometric Persistence/Weak Persistence	0.9673
`layer_transition_code`	Geometric Persistence/Weak Persistence	0.9537

An important nuance is that raw total-charge encodings (`initial_total_charge`, `final_total_charge`) become less structurally decisive as the corpus expands (dropping from Geometric Persistence/Weak Persistence in Phase 3 to Structural Boundary/Transitional Structure in Phase 3B). This is consistent with the hypothesis that charge conservation is a necessary but not sufficient structural description: the persistent geometry concentrates in route, closure, category, class, family, and layer transition coordinates.

Finding 10.1. The Phase 3B expansion shows that route and closure persistence is not a seven-transition artifact. Route and closure transition encodings advance to Boundary-Stabilized with $\langle A_\kappa \rangle > 0.975$ across 38 transitions spanning 8 decay families. Raw total-charge coordinates become less structurally decisive as the corpus grows, further concentrating the persistent signal in the route/closure geometry.

11 Phase 3C Results: Forbidden and Constrained Transition Boundary Tests

11.1 Contrast-corpus design

Phase 3C tests the boundary side of Charge Boundary Routing. Whereas Phases 3 and 3B contain allowed transitions, Phase 3C mixes allowed controls with forbidden, constrained, free-fractional, and route-incoherent candidates. The 48-row corpus contains 12 allowed controls, 8 charge-violating mock transitions, 8 free-fractional externalization attempts, 8 selection-rule violating comparison channels, 8 route-incoherent charge-conserving mocks, and 4 constrained boundary cases. The design deliberately includes both direct charge-balance violations and charge-balanced route-incoherent cases. The latter are the decisive UNNS test: they ask whether $Q_i = Q_f$ can hold while route / closure admissibility fails.

11.2 STRUC-PERC-I: connected mixed boundary corpus

STRUC-PERC-I shows that the Phase 3C corpus does not fragment as a graph. Of 43 submitted ladders, 42 produced completed results and all 42 reached FULL_PERCOLATION. No completed ladder reached HARD_FRAGMENTATION, and no isolated nodes or tail-dominant components were observed. One low-information control file (`allowed_control_flag`) produced no result and is excluded from the verdict count. The mixed allowed / forbidden / constrained corpus therefore remains globally connected across all completed encodings.

This result is important because it shows that forbiddenness is not expressed as simple graph disconnection. The boundary distinction must be read at the perturbative admissibility level.

11.3 STRUC-I: route-transition admissibility collapse

STRUC-I supplies the decisive contrast. Across 43 parsed ladders, only 8 reached Geometric Persistence, while 35 fell to Structural Boundary. The state distribution was 3 Boundary-Stabilized, 5 Weak Persistence, 33 Transitional Structure, and 2 Near-Critical. The mixed Phase 3C corpus is therefore connected but largely boundary-transitional.

The most important change occurs in `route_transition_code`. In Phase 3B, the allowed-transition corpus made `route_transition_code` Boundary-Stabilized with $\langle A_\kappa \rangle = 0.9851$. In Phase 3C, `route_transition_code` falls to Structural Boundary / Transitional Structure with $\langle A_\kappa \rangle = 0.859$ and $\min A_\kappa = 0.814$. `transition_status_code` also remains Structural Boundary / Transitional Structure with $\langle A_\kappa \rangle = 0.886$, and `boundary_pressure_index` remains Structural Boundary / Transitional Structure with $\langle A_\kappa \rangle = 0.918$.

This shows that Phase 3C does not merely add new labels to the transition space. It drives the route-transition coordinate below the Geometric Persistence threshold.

Exact values:

- `route_transition_code`: $\langle A_\kappa \rangle = 0.859$, $\min A_\kappa = 0.814$; Structural Boundary /

Transitional Structure.

- `transition_status_code`: $\langle A_\kappa \rangle = 0.886$, $\min A_\kappa = 0.862$; Structural Boundary / Transitional Structure.
- `boundary_pressure_index`: $\langle A_\kappa \rangle = 0.918$, $\min A_\kappa = 0.876$; Structural Boundary / Transitional Structure.

11.4 Free-fractional externalization threshold pressure

Phase 3C also reveals threshold pressure in free-fractional externalization encodings. Although these encodings reach full_percolation, they connect at substantially higher thresholds than most route / status encodings. In particular, `free_fractional_externalization_flag` connects at $\kappa_{\text{conn}} \approx 0.750$, while `boundary_pressure_index` connects at $\kappa_{\text{conn}} \approx 0.562$. These contrast with the many primary encodings that connect at $\kappa_{\text{conn}} \approx 0.010$.

This indicates that free-fractional externalization does not break the transition graph, but it requires stronger tolerance to join the connected structure. This is consistent with the interpretation that fractional charge is a confined internal route coordinate and that attempted free-fractional externalization belongs to the boundary side of the system.

11.5 Phase 3B vs Phase 3C comparison

The contrast with Phase 3B is the key result (Table 6). Phase 3B allowed transitions stabilize both route and closure transition geometry. Phase 3C preserves closure, category, and family classification, but `route_transition_code` collapses from Boundary-Stabilized to Transitional Structure. Thus the boundary is not a loss of all structure. It is a selective loss of route-transition admissibility.

Finding 11.1. Phase 3C completes the allowed / forbidden contrast. The mixed allowed / forbidden / constrained corpus remains globally connected under STRUC-PERC-I (42/42 full_percolation, 0 hard_fragmentation), but STRUC-I drives `route_transition_code` into Structural Boundary / Transitional Structure ($\langle A_\kappa \rangle = 0.859$). Forbiddenness therefore appears not as graph disconnection, but as boundary pressure in perturbative route geometry. Charge balance is necessary but not sufficient: route-transition admissibility distinguishes allowed transitions from charge-balanced but structurally incoherent transformations.

12 Discussion

12.1 Charge as projection

The completed six-phase program produces a coherent reframing of charge. Charge value Q is necessary; it enters conservation laws, determines coupling to electromagnetic fields, and is experimentally accessible. But Q alone is insufficient to characterize a charge-bearing system in the tested corpus. The route coordinate carries information that Q does not.

The positron and the W^+ share $Q/e = +1$. But the positron is an external lepton closure and the W^+ is an external gauge-sector closure. They are in the same layer and same route class, but in different physical sub-categories. The proton shares $Q/e = +1$ with both of them, but it is a composite baryon closure—a qualitatively different route. The scalar Q collapses all three onto a single point. The route tuple distinguishes them.

12.2 Fractional charge as a confined internal route coordinate

Layer B reframes the fractional charge question. Standard approaches ask why $\pm 1/3$ and $\pm 2/3$ do not appear as free external charges. The UNNS charge-routing answer is: because fractional charge is represented as a confined internal route coordinate, not as a failed external charge.

The BC bridge result supports this interpretation directly. The fractional-to-composite bridge percolates in route and closure coordinates: the route system is connected across the B-to-C transition. What the BC bridge shows is not confinement (which is a dynamic QCD result) but a structural fact: fractional and composite coordinates are route-connected in the charge-routing topology.

12.3 Composite charge as closure

Layer C shows that composite charge is a structural operation, not merely arithmetic. A proton is not defined by the equation $\frac{2}{3} + \frac{2}{3} - \frac{1}{3} = 1$. That equation gives the correct value, but it omits the structural operation: three confined fractional route coordinates close into a single external integer state.

The UNNS representation captures this as a route from **Layer B** to **Layer C**: internal fractional coordinates $\rightarrow$ composite closure boundary $\rightarrow$ external projection $= +1$. The charge value is the last step of this route, not the whole story.

12.4 Boundary absence as structure

Layer D is perhaps the most conceptually distinctive contribution. In standard treatments, the non-observation of free quarks is a negative experimental result and the non-observation of magnetic monopoles is a constraint from searches. In the UNNS charge-routing framework, these absences are positive structural objects: they mark where the routing system refuses to externalize certain charge configurations.

The CD and BCD bridges fragment entirely when Layer D is added. This is not a failure of the framework; it is the framework detecting a genuine topological boundary. Layer D is the terminus of the charge route, not a gap in the corpus.

12.5 Allowed transitions as route-preserving transformations

Phase 3 and Phase 3B reframe what an allowed transition *is*. The scalar conservation statement $Q_i = Q_f$ is necessary but not sufficient. Allowed transitions also preserve route and closure transition structure.

The `route_transition_code` and `closure_transition_code` encodings are the strongest STRUC-I coordinates in Phase 3B, reaching Boundary-Stabilized. This means the route/closure transition geometry is not only present but admissibility-stable under perturbation of the transition corpus. An allowed transition is a route-preserving transformation.

12.6 Forbiddenness as admissibility-boundary pressure

Phase 3C refines the interpretation of transition admissibility. The forbidden / constrained corpus does not disconnect under STRUC-PERC-I; it remains globally connected. However, the route-transition coordinate falls below the Geometric Persistence threshold under STRUC-I. This shows that the forbidden boundary is not a crude graph-theoretic separa-

tion. It is a perturbative admissibility boundary. Coarse closure and category labels remain stable, but admissible route transition is lost.

12.7 Relation to the UNNS library

This manuscript is a physical-domain specialization of several prior UNNS results. It operationalizes admissibility geometry in the electric charge domain, demonstrating that a physical quantity can be studied as a routed boundary structure. The Margin-Confinement Law [2] established the hard-boundary invariant; Admissible Cluster Geometry [3] mapped internal basin topology; and Admissible Boundary Routing [4] introduced route-topology analysis in the cosmological domain. The bridge geometry methodology is extended here from the stellar domain [5] to particle physics. The same-charge control is structurally analogous to the finding across those corpora that basin co-occupancy does not imply structural equivalence.

The charge routing framework supports a general UNNS principle: *value is projection; route is structure; closure is admissibility; and forbiddenness is boundary pressure in route geometry.*

13 Relation to Existing Theories

13.1 Relation to the Standard Model

The Standard Model encodes electric charge through U(1) gauge structure, hypercharge, weak isospin, and the Gell-Mann–Nishijima relation. It provides the correct charge assignments and predicts all measured charges with extraordinary precision.

Charge Boundary Routing does not replace this. It adds a structural classification layer: given that the Standard Model assigns a charge value to each particle, the UNNS framework asks how charge-bearing systems group into route classes, closure states, and admissibility structures. The relation is complementary. The Standard Model provides the physical mechanism; the UNNS framework provides the boundary-route classification.

A concrete illustration of complementarity is the BC bridge result (Section 7). The Standard Model assigns $+2/3$ and $-1/3$ to quarks and $+1$ to the proton via QCD color confinement. The UNNS BC bridge shows that, at the structural route level, the fractional-to-composite layer interface is route-connected (all route and closure encodings reach Full Percolation) while signed charge fragments. This is not a contradiction of the Standard Model; it is a complementary structural observation: the route topology is better connected than the charge-value topology at this interface.

13.2 Relation to U(1) charge conservation

In conventional field theory, electric charge conservation follows from U(1) gauge symmetry via Noether's theorem. This gives a precise statement of the conservation law and explains it through symmetry.

Charge Boundary Routing does not derive U(1). It reframes what U(1) conserves: U(1) expresses the symmetry that ensures $Q_i = Q_f$; UNNS route preservation describes how charge-bearing structures remain admissible across closure transformations. The two statements are compatible. U(1) operates at the level of field representations; UNNS boundary-route preservation operates at the level of structural classification.

13.3 Relation to quark confinement

Quantum chromodynamics explains quark confinement through the behavior of the strong force at large distances. The UNNS charge-routing framework does not prove confinement. It represents confinement as a boundary-routing condition: Layer B (confined fractional coordinates) does not cross into the domain of free external closure states, and Layer D marks the boundary objects where free fractional externalization is absent.

This is a structural description of what QCD explains dynamically. The two descriptions are not in conflict. We represent confinement as a boundary-routing condition; QCD explains the mechanism that enforces it.

13.4 Relation to the quark model and composite hadrons

The quark model computes hadron charges as arithmetic sums of constituent quark charges. The UNNS framework adds: composite charge is closure, not merely summation. A proton is an admissible composite closure whose external projection is $+1$; the arithmetic $+2/3 + 2/3 - 1/3 = +1$ describes the projection, not the closure operation.

This distinction matters structurally: the BC bridge results show that the fractional-to-composite transition is route-connected, not merely a charge-addition step.

13.5 Relation to decay and transition selection rules

Standard decay selection rules specify which transitions are allowed based on conservation of charge, baryon number, lepton number, parity, and other quantum numbers. Charge Boundary Routing adds that allowed transitions also preserve route and closure transition structure. Phase 3B shows the positive side empirically: among 38 allowed transitions spanning 8 decay families, route and closure transition encodings reach Boundary-Stabilized—the strongest admissibility signal in the corpus. Phase 3C then supplies the contrast: forbidden, constrained, and route-incoherent candidates remain percolatively connected but degrade route-transition admissibility. This is compatible with standard selection rules and re-expresses them as a boundary distinction in route geometry rather than as a replacement for quantum field theory.

13.6 Relation to topology and percolation

STRUC-PERC-I frames the charge corpus as a percolation problem. Which encodings form a connected graph and which fragment? The finding that charge-value encodings can fragment while route/closure encodings percolate is topologically significant: the chosen coordinate system changes the visible connectedness of the charge corpus.

This connects to broader results in topological data analysis showing that the "right" coordinate system for a dataset depends on what structural relationships one wishes to preserve.

13.7 Relation to admissibility geometry

STRUC-I identifies which encodings are perturbatively stable within the UNNS admissibility manifold $\mathcal{M}_{\text{adm}}$. The same-charge control shows that structural route and subtype pair encodings can achieve Stable Structure even when charge equality itself is trivial. The transition phases show that route/closure transitions reach Boundary-Stabilized admissibility. These results connect the charge-routing program to the broader UNNS admissibility geometry developed in companion manuscripts [2, 3, 4, 5].

Phase 3C shows that the admissibility manifold can remain connected while losing perturbative route stability. This separates connectivity from admissibility and strengthens the interpretation of STRUC-I as a boundary detector rather than a graph-connectivity measure.

14 Limitations

The following limitations apply to the present work.

1. **No derivation of e.** This work does not derive the unit charge e or explain charge quantization from first principles. The corpus takes charge values as given from experimental data.
2. **No replacement of U(1) gauge theory.** The charge-routing framework is a structural classification layer. It does not replace or subsume U(1) electromagnetism.
3. **No proof of confinement.** Quark confinement is represented as a boundary-routing condition but is not derived.
4. **No derivation of the Standard Model.** The Standard Model particle content and charge assignments are taken as input, not output.
5. **Categorical codes are not physical magnitudes.** The integer codes used for route class, closure class, transition type, and related categorical attributes are structural encodings. Their numeric values are classification labels, not physical quantities.
6. **The Phase 3B transition corpus is not exhaustive.** 38 transitions across 8 decay families constitute a controlled robustness corpus, not a complete particle-decay database. Results are scoped to the tested corpus.
7. **Phase 3C forbidden / constrained corpus is controlled, not exhaustive.** Phase 3C includes 48 deliberately constructed boundary tests across allowed controls, charge-violating mocks, free-fractional externalization attempts, selection-rule violating comparisons, route-incoherent charge-conserving mocks, and constrained boundary cases. It is a controlled contrast corpus, not a complete catalogue of all forbidden or constrained transitions.
8. **Mock transitions are diagnostic constructs.** Some Phase 3C rows are deliberately constructed mock transitions. Their purpose is not to propose physical processes, but to test whether charge balance can be separated from route / closure admissibility.
9. **Phase 3C does not derive selection rules.** The result shows boundary-pressure signatures in the tested corpus; it does not derive Standard Model selection rules or replace quantum field theory.
10. **The Layer D chamber rejection is informative, not a limitation.** The non-runnability of Layer D as a standard numeric ladder is a diagnostic finding, not a gap. Layer D is a boundary-condition layer that resists ordinary percolation analysis.
11. **Pilot corpus scope.** All claims are scoped to the tested corpus. Phrases such as "in the tested corpus" and "within the UNNS Substrate representation" apply throughout.

15 Next Work

With Phase 3C complete, the next work is to deepen and validate the forbidden boundary result. Three directions follow.

1. **Phase 3D — expanded forbidden / constrained corpus.** Expand Phase 3C from 48 rows to 72–96 rows and separate mock, constrained, and physically searched channels more finely.
2. **Phase 3C-A — ablation and group-isolated tests.** Run allowed-only, charge-violating-only, free-fractional-only, route-incoherent-only, and constrained-only chamber batches to determine which group drives route-transition collapse.
3. **Physics-aligned refinement.** Replace selected mock rows with more tightly sourced PDG upper-bound channels and selection-rule examples, preserving the same corpus schema.

The goal is not to change the Phase 3C conclusion, but to localize the boundary mechanism more sharply.

16 Conclusion

Charge Boundary Routing I establishes a routed view of electric charge.

The completed six-phase empirical program shows that the charge-bearing corpus separates into four structurally distinct layers: external free closure states (**Layer A**), confined fractional coordinates (**Layer B**), composite closures (**Layer C**), and boundary absences (**Layer D**). Bridge geometry between layers reveals that charge-value encodings and route/closure encodings produce genuinely different topological behavior: the same corpus fragments in charge-value space and percolates in route/closure space.

A pairwise same-charge control demonstrates that $Q/e = +1$ does not imply the same structural route. With charge equality fixed by construction, the route encoding reaches Stable Structure ($A_\kappa = 1.000$) while the charge equality encoding remains Transitional.

Allowed transitions—7 in the seed corpus, 38 in the expanded robustness corpus—preserve route and closure transition structure beyond total charge balance. The route and closure transition encodings advance from Weak Persistence to Boundary-Stabilized as the corpus expands, confirming that the result is not a seed-corpus artifact.

Phase 3C completes the allowed / forbidden contrast. A 48-row mixed corpus of allowed controls, charge-violating mocks, free-fractional externalization attempts, selection-rule violating comparisons, route-incoherent charge-conserving mocks, and constrained boundary cases remains globally connected under STRUC-PERC-I. However, under STRUC-I the `route_transition_code` encoding falls to Structural Boundary / Transitional Structure, with $\langle A_\kappa \rangle = 0.859$. Closure, category, and family labels remain stable, but route-transition admissibility is lost. This shows that the boundary is not simple graph disconnection, but perturbative route-geometry pressure in the admissibility manifold.

The project offers a structural reframing of five charge concepts:

- *Fractional charge* is a confined internal route coordinate, not a failed external charge.
- *Composite charge* is closure, not merely summation.

- *Boundary absence* is structural, not simply missing data.
- *Allowed transitions* preserve route and closure structure beyond scalar charge balance.
- *Forbidden and constrained transition candidates* can remain connected while losing route-transition admissibility.

The manuscript does not replace the Standard Model, prove confinement, or derive the value of e. It establishes a structural language in which these phenomena can be expressed as routing, closure, and boundary conditions within an admissibility geometry.

Principle 16.1 (Final)**.** Charge is conserved as a value, but structured as a route. The final principle of Charge Boundary Routing I is:

Charge conservation is the visible projection; boundary-route preservation is the structural invariant; charge balance is necessary but not sufficient.

Tables

Table 1: Layered corpus summary. All 40 objects are PDG-sourced or PDG-aligned from RPP 2026. Route class and closure class are UNNS structural encodings, not physical magnitudes.

Layer	Structural Role	Count	Example Objects	UNNS Interpretation
A	External/free closure states	14	$e^{\pm}$, $\mu^{\pm}$, $\tau^{\pm}$, $\nu_{e,\mu,\tau}$, γ, $W^{\pm}$, Z^0, H	Free external charge expression; 8 `FREE_INTEGER`, 6 `FREE_NEUTRAL`
B	Confined fractional coordinates	12	u, d, s, c, b, t and antiquarks	Internal route coordinates; not externally free; all `INTERNAL_FRACTIONAL`
C	Composite closures	10	p, n, Δ^{++}, Ω^{-}, $\pi^{\pm}$, π^0, $K^{\pm}$, K^0	Fractional internal coordinates close into integer or neutral external state
D	Boundary absences/constraints	4	Free quark (absent), monopole (absent), charge-violation mode (bounded), neutrality constraint	Boundary conditions of the routing system; not failed rows

Table 2: Phase sequence summary. Each phase addresses a distinct charge-boundary question, and together they form a coherent empirical chain.

Phase	Corpus/Test	Chamber Input	Main Result	Interpretation
1	40 objects, Layers A–D	6 ladder encodings per layer	Corpus separates into 4 structural layers	Charge-bearing objects occupy distinct route regimes
2	5 bridge corpora (AB, BC, CD, ABC, BCD)	6 encodings per bridge	Charge-value and route/closure topology differ	CD and BCD fragment; BC route-connected
2C-P	5 objects × $\binom{5}{2} = 10$ pairs, $Q/e = +1$	27 pairwise encodings	Route pair codes: Stable Structure ($A_\kappa = 1.000$)	Same charge does not imply same route
3	7 seed transitions	10 transition encodings	Route/closure transition: Weak Persistence	Allowed transitions preserve route/closure geometry
3B	38 allowed transitions, 8 families	21 transition encodings	Route/closure: Boundary-Stabilized ($A_\kappa \approx 0.985$)	Transition result is not a seed-corpus artifact
3C	48 mixed boundary tests, 6 groups (A: allowed controls, B: charge-violating, C: free-fractional, D: selection-violation, E: route-incoherent, F: constrained)	43 encodings	42/42 FP; route_trans.: SB/TS ($A_\kappa = 0.859$); closure_trans.: GP/BS ($A_\kappa = 0.998$)	Forbiddenness as route-admissibility pressure, not graph disconnection

Table 3: Bridge geometry outcomes under STRUC-PERC-I v2.5.0. FP = Full Percolation; HF = Hard Fragmentation. Charge-value encodings: absolute charge and signed charge. Route/closure encodings: boundary route coordinate, closure class, closure state, route class.

Bridge	Layers	Charge-value	Route/closure	Interpretation
AB	A ↔ B	Both HF (GR 0.75, 0.857)	3/4 FP, all κ_{conn} low	Magnitude stable; charge-value fragments; route percolates
BC	B ↔ C	Abs. charge FP ($\kappa_{\text{conn}} = 1$); signed charge HF (GR 0.857)	All FP	Route-connected fractional-to-composite bridge
CD	C ↔ D	n/a (no charge ladder for D)	All 4 HF (GR 0.833–0.900)	Layer D terminates the route; boundary fragmentation
ABC	A, B, C	Abs. charge FP; signed charge HF (GR 0.857); boundary route HF (GR 0.667)	Closure class, state, route class: all FP	Composite-mediated partial recovery; transitional
BCD	B, C, D	n/a	All 4 HF (GR 0.778–0.900)	Terminal boundary extension; Layer D enforces fragmentation

Table 4: Same-charge route control results (**Phase 2C-P**). All 10 pairs have $\Delta Q = 0$ by construction. Persistent signals in structural encodings reflect route separation, not charge variation. All 27 encodings: STRUC-PERC-I verdict = Full Percolation.

Encoding	PERC	STRUC-I State	$\langle A_\kappa \rangle$	Interpretation
structural_route_pair_code	FP	Geometric Persistence/Stable Structure	1.000	Maximum stability; route separation fully persistent
sub_category_pair_code	FP	Geometric Persistence/Stable Structure	1.000	Sub-category difference persistent at maximum
category_pair_code	FP	Geometric Persistence/Weak Persistence	1.000	Category pair code: strong, below stable threshold
layer_difference	FP	Geometric Persistence/Weak Persistence	0.942	Layer difference persistent
closure_class_difference	FP	Geometric Persistence/Weak Persistence	0.941	Closure class difference persistent
route_class_difference	FP	Geometric Persistence/Weak Persistence	0.941	Route class difference persistent
charge_difference	FP	Structural Boundary/Transitional Structure	0.863	Trivial control (constant = 0); correctly transitional
same_charge_pair	FP	Structural Boundary/Transitional Structure	0.860	Trivial control (constant = 1); correctly transitional
structural_distance	FP	Structural Boundary/Transitional Structure	0.780	Aggregate distance below persistence threshold
type_distance	FP	Structural Boundary/Transitional Structure	0.771	Type distance below persistence threshold

Table 5: Phase 3 seed and Phase 3B expanded transition results. "Ph.3 PERC" and "Ph.3B PERC" give STRUC-PERC-I verdicts (FP = Full Percolation, HF = Hard Fragmentation). $\langle A_\kappa \rangle$ values from STRUC-I. BS = Boundary-Stabilized; WP = Weak Persistence; TS = Transitional.

Encoding	P3 PERC	P3 STRUC-I	P3B PERC	P3B STRUC-I	Interpretation
route_transition_code	FP	0.9999 (WP)	FP	0.9851 (BS)	Strongest signal; advances to Boundary-Stabilized
closure_transition_code	FP	0.9999 (WP)	FP	0.9839 (BS)	Equally strong; Boundary-Stabilized
transition_class_code	FP	0.9999 (WP)	FP	0.9775 (BS)	Class geometry: Boundary-Stabilized
category_transition_code	—	—	FP	0.9776 (BS)	Category: Boundary-Stabilized in Phase 3B
transition_family_code	—	—	FP	0.9673 (WP)	Family: Weak Persistence
layer_transition_code	FP	— (TS)	FP	0.9537 (WP)	Advances from Transitional to Weak Persistence
initial_total_charge	FP	0.9575 (WP)	FP	— (TS)	Raw charge weakens as corpus expands
final_total_charge	FP	0.9565 (WP)	FP	— (TS)	Raw charge weakens as corpus expands
charged_multiplicity_delta	**HF**	— (TS)	FP	— (TS)	Seed fragmentation: small-corpus sensitivity

Table 6: Phase 3B vs Phase 3C transition-boundary comparison under STRUC-I. Phase 3B contains 38 allowed transitions; Phase 3C contains 48 mixed allowed, forbidden, constrained, free-fractional, and route-incoherent candidates. The decisive contrast is route_transition_code: Boundary-Stabilized in Phase 3B, Structural Boundary / Transitional in Phase 3C. Closure, category, and family labels remain stable across the contrast.

Encoding	3B State	$\langle A_\kappa \rangle_{3B}$	3C State	$\langle A_\kappa \rangle_{3C}$	Interpretation
route_transition_code	GP/BS	0.9851	SB/TS	0.859	Route admissibility collapses in boundary corpus
closure_transition_code	GP/BS	0.9839	GP/BS	0.998	Closure labels remain stable
category_transition_code	GP/BS	0.9776	GP/BS	0.994	Category remains stable
transition_family_code	GP/WP	0.9673	GP/BS	0.988	Family classification remains stable
boundary_pressure_index	—	—	SB/TS	0.918	Boundary pressure below persistence threshold
transition_status_code	—	—	SB/TS	0.886	Allowed/forbidden status transitional

Figures

A Corpus Encodings: Phase 1 Ladder Attributes

Each Phase 1 corpus object is encoded with the following attributes, which serve as ladder dimensions for the two chambers.

A.1 Charge-value encodings

`absolute_charge` $|Q/e|$: the unsigned magnitude of the external charge. Takes values in $\{0, 1/3, 2/3, 1, 2\}$ for the Phase 1 corpus.

`signed_charge` Q/e: the signed external charge. Takes values in $\{-2, -1, -2/3, -1/3, 0, +1/3, +2/3, +1, +2\}$.

A.2 Route/closure encodings

`boundary_route_coordinate` Integer code identifying the route topology: external closure (1), confined route (2), composite closure (3), boundary absence (4), dual boundary (5).

`closure_class_code` Integer code for the closure class (9 values; see Section 3).

`closure_state_code` Integer code for the closure state (whether the external charge is integer, neutral, fractional, or absent).

`route_class_code` Integer code for the route class (EXTERNAL_CLOSURE, CONFINED_ROUTE, COMPOSITE_CLOSURE, BOUNDARY_ABSENCE, DUAL_BOUNDARY_CANDIDATE, BOUNDARY_CONSTRAINT).

A.3 Pairwise control encodings (Phase 2C-P)

All Phase 2C-P encodings are computed over pairs (i, j) of the five $Q/e = +1$ control objects:

- Difference encodings: $|x_i - x_j|$ for categorical code x (layer, category, sub-category, route class, closure class, structural route, composite, external, fermion, boson, hadron, meson, baryon, lepton, gauge boson).
- Pair-code encodings: combined pair identifiers (layer pair code, category pair code, sub-category pair code, route class pair code, closure class pair code, structural route pair code, pair class code).
- Distance encodings: type distance, route distance, structural distance.
- Control encodings: charge difference (constant = 0), same charge pair (constant = 1).

A.4 Transition encodings (Phases 3, 3B, and 3C)

`route_transition_code` Integer encoding the route-class pair of initial and final states.

`closure_transition_code` Integer encoding the closure-class pair.

`category_transition_code` Integer encoding the particle-category pair.

`transition_class_code` Integer encoding the transition type (composite-to-composites, composite-to-externals, external-to-externals, etc.).

`transition_family_code` Integer encoding the decay family (baryon decay, charged meson decay, W/Z channel, etc.).

`layer_transition_code` Integer encoding the layer-pair of initial and final states.

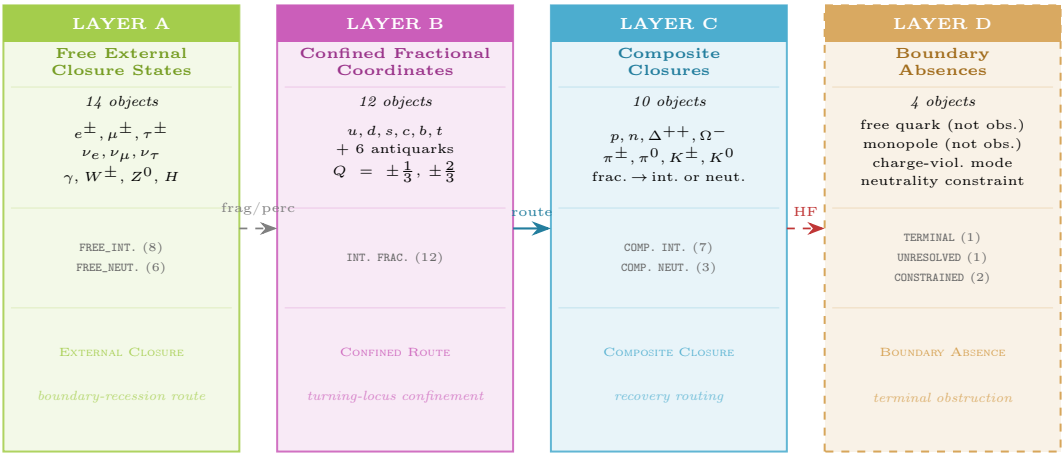

Figure 1: Four-layer charge-boundary architecture. Layers A–D, left to right, with colored headers and dashed border (Layer D) indicating boundary-terminus status. **A** (green): 14 external/free closure states; **B** (magenta): 12 confined fractional quark coordinates; **C** (cyan): 10 composite hadron closures; **D** (amber, dashed): 4 boundary absences or constraints. Arrows encode inter-panel bridge topology: frag/perc (AB: charge-value fragments while route percolates); route (BC: route-connected); HF (CD: all encodings fragment — boundary terminus). π^0 is a composite neutral meson in Layer C, not a primitive closure.

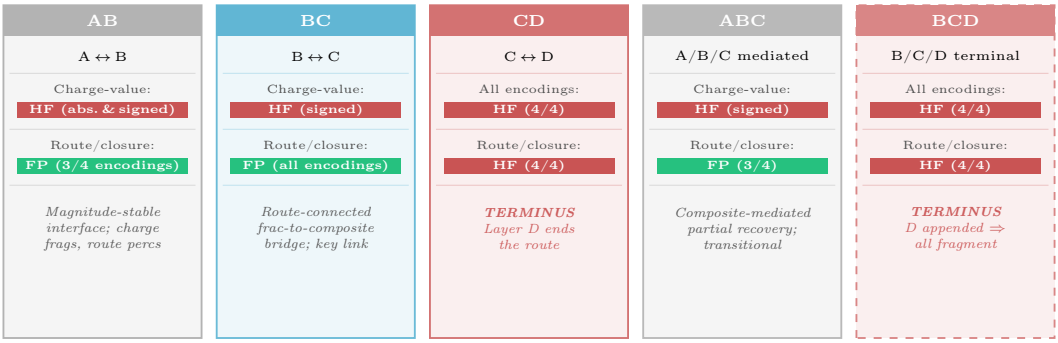

Figure 2: Bridge geometry map (Phase 2). Five bridge corpora spanning adjacent or multi-spanning layers. Green (FP) indicates Full Percolation; red (HF) indicates Hard Fragmentation. The BC bridge is route-connected (FP across all route/closure encodings) while signed charge fragments. CD and BCD are topological termini: Layer D causes global Hard Fragmentation at every interface it touches. The key finding: charge-value topology and route/closure topology are not equivalent across the tested layer interfaces.

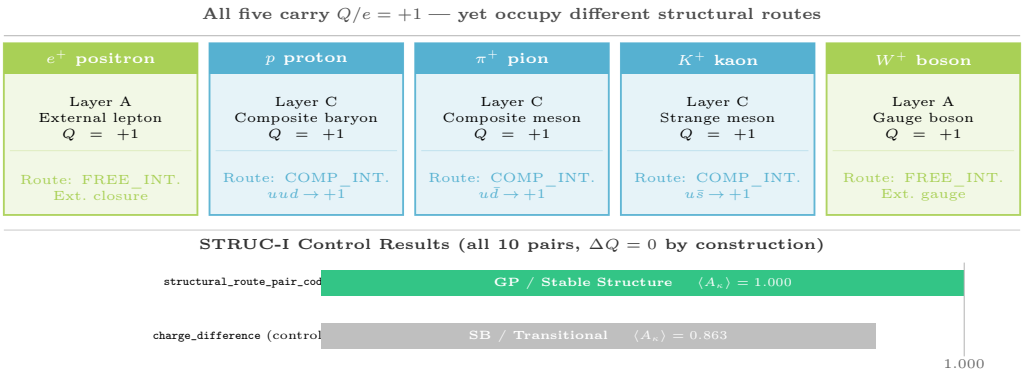

Figure 3: Same-charge route control (Phase 2C-P). *Top:* Five objects all carrying $Q/e = +1$ occupy different structural routes, layers, and physical categories (external lepton, composite baryon, composite meson, strange meson, external gauge boson). *Bottom:* STRUC-I results for the 10 unordered pairs ($\Delta Q = 0$ for all pairs by construction). `structural_route_pair_code` reaches Geometric Persistence / Stable Structure ($\langle A_\kappa \rangle = 1.000$), while the trivial same-charge control encoding (`charge_difference`) remains Structural Boundary / Transitional ($\langle A_\kappa \rangle = 0.863$). The persistent signal is route separation, not charge detection.

ID	Process	ΔQ	route_transition_code $\langle A_\kappa \rangle$
T001	neutron β-decay: $n \to p + e^- + \bar{\nu}_e$	0 ✓	GP / Weak Persistence 0.9999
T002	π^+ muonic: $\pi^+ \to \mu^+ + \nu_\mu$	0 ✓	GP / Weak Persistence 0.9999
T003	μ^- decay: $\mu^- \to e^- + \bar{\nu}_e + \nu_\mu$	0 ✓	GP / Weak Persistence 0.9999
T004	W^- leptonic: $W^- \to e^- + \bar{\nu}_e$	0 ✓	GP / Weak Persistence 0.9999
T005	W^+ leptonic: $W^+ \to e^+ + \nu_e$	0 ✓	GP / Weak Persistence 0.9999
T006	π^0 two-photon: $\pi^0 \to \gamma + \gamma$	0 ✓	GP / Weak Persistence 0.9999
T007	K^+ muonic: $K^+ \to \mu^+ + \nu_\mu$	0 ✓	GP / Weak Persistence 0.9999

* *charged_multiplicity_delta: HF in seed (diagnostic; resolves in Phase 3B)*

Figure 4: Seed transition dynamics (Phase 3, $n = 7$). Seven canonical allowed charge-conserving transitions, all with $\Delta Q = 0$ (verified). `route_transition_code` and `closure_transition_code` reach Geometric Persistence / Weak Persistence ($\langle A_\kappa \rangle = 0.9999$) under STRUC-I. The single Hard Fragmentation outcome (`charged_multiplicity_delta`, GR = 0.857) is diagnostically meaningful: allowed transitions are not organized by charged-object count change. This fragmentation resolves in Phase 3B (Figure 5).

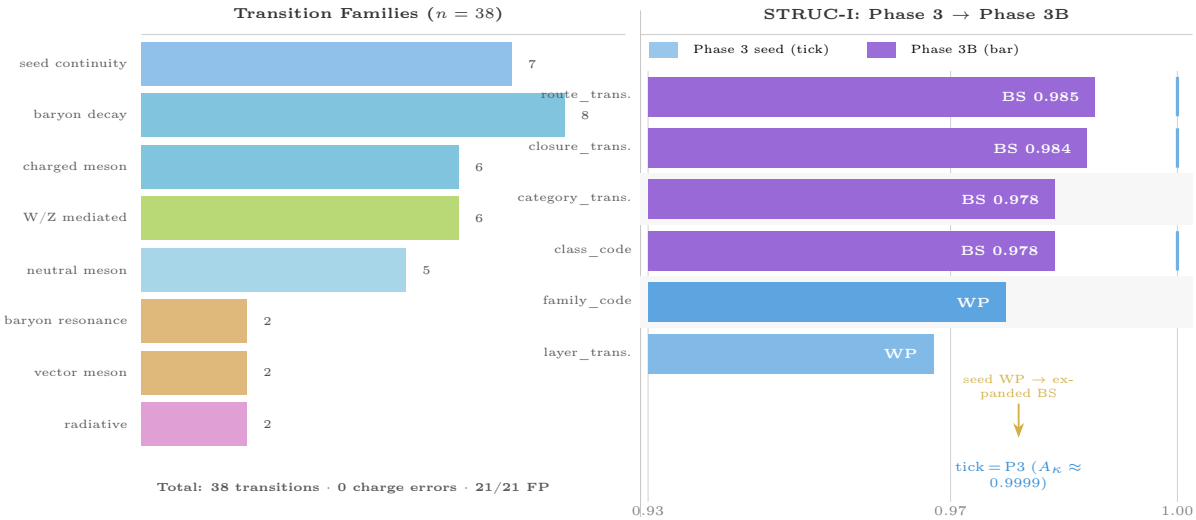

Figure 5: Phase 3B expansion robustness. *Left:* 38 allowed transitions across 8 decay families. *Right:* STRUC-I $\langle A_\kappa \rangle$ for key transition encodings. Vertical ticks show Phase 3 seed ($\langle A_\kappa \rangle \approx 0.9999$, WP). Filled bars show Phase 3B expanded values. Route and closure encodings advance from Weak Persistence to Boundary-Stabilized (BS). Category and class encodings also reach BS. All 21/21 STRUC-PERC-I encodings: Full Percolation; 0 Hard Fragmentation.

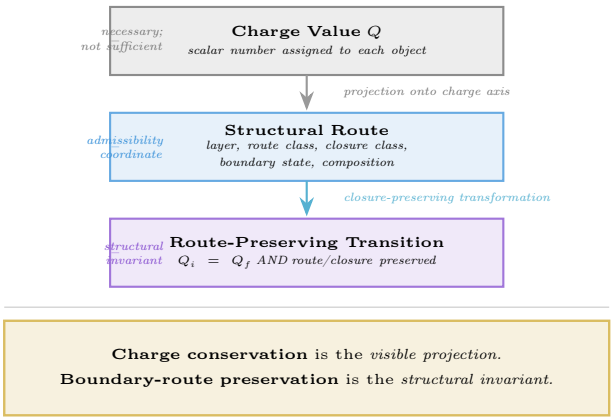

Figure 6: Integrated principle of Charge Boundary Routing. The scalar charge value Q is a projection onto the observable charge axis — necessary but insufficient to characterize a charge-bearing system. The structural route (a multi-coordinate tuple covering layer, route class, closure class, boundary state, and composition status) is the admissibility coordinate. Allowed transitions are not merely $Q_i = Q_f$; they are closure-preserving transformations that carry route structure from initial to final state. The final principle: charge is conserved as a value but structured as a route.

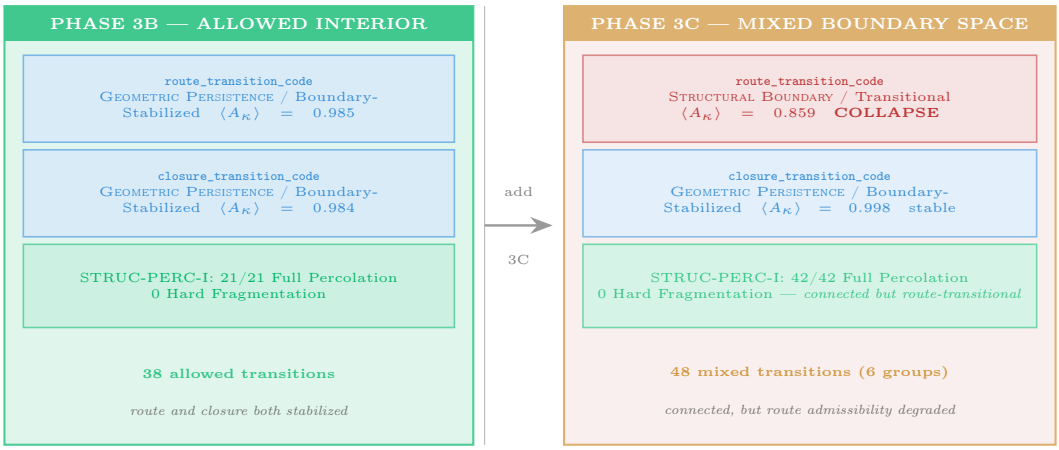

Figure 7: Allowed interior vs. forbidden boundary (Phase 3B / Phase 3C contrast). Phase 3B: 38 allowed transitions; both `route_transition_code` and `closure_transition_code` reach Geometric Persistence / Boundary-Stabilized. Phase 3C: 48 mixed allowed / forbidden / constrained candidates; the corpus remains globally connected under STRUC-PERC-I (42/42 Full Percolation), but `route_transition_code` collapses to Structural Boundary / Transitional Structure ($\langle A_\kappa \rangle = 0.859$) while `closure_transition_code` remains Boundary-Stabilized ($\langle A_\kappa \rangle = 0.998$). Forbiddenness appears not as graph disconnection but as selective loss of route-transition admissibility.

`initial_total_charge` Scalar: $\sum_i Q_i/e$ for initial particles.

`final_total_charge` Scalar: $\sum_f Q_f/e$ for final particles.

`charge_balance_error` $|\sum_i Q_i - \sum_f Q_f|/e$: zero for all 38 Phase 3B transitions.

`charged/neutral multiplicity delta` Change in number of charged/neutral particles.

`composite/external count delta` Change in composite or external object count.

`externalization_delta` Change in number of external-layer particles.

B Chamber Result Summaries

B.1 Phase 1: ABCD combined STRUC-PERC-I

Encoding	Verdict	GR	Isolated	κ_{conn}
absolute_charge	HF	0.750	1	—
signed_charge	HF	0.857	1	—
boundary_route_coordinate	FP	1.000	0	1.000
closure_class_code	FP	1.000	0	1.000
closure_state_code	FP	1.000	0	0.010
route_class_code	FP	1.000	0	0.010

B.2 Phase 1: ABCD combined STRUC-I

Encoding	Regime	State	$\langle A_\kappa \rangle$	$\min A_\kappa$
route_class_code	SB	TS	0.9194	0.8980
closure_class_code	SB	TS	0.8814	0.8490
boundary_route_coordinate	SB	TS	0.8804	0.8475
closure_state_code	SB	TS	0.8738	0.8485
absolute_charge	SB	TS	0.8657	0.8430
signed_charge	SB	TS	0.6574	0.5845

B.3 Phase 2C-P: Top and bottom STRUC-I encodings

Encoding	State	$\langle A_\kappa \rangle$	$\min A_\kappa$
structural_route_pair_code	GP/Stable	1.000	1.000
sub_category_pair_code	GP/Stable	1.000	1.000
category_pair_code	GP/Weak	1.000	1.000
baryon_difference	GP/Weak	0.943	0.933
layer_difference	GP/Weak	0.942	0.932
...			
structural_distance	SB/TS	0.780	0.688
category_difference	SB/TS	0.751	0.698
type_distance	SB/TS	0.771	0.678
charge_difference	SB/TS	0.863	0.833
same_charge_pair	SB/TS	0.860	0.840

B.4 Phase 3B: Full STRUC-PERC-I table (21/21 FP)

All 21 encodings reach FULL_PERCOLATION with GR = 1.000 and isolated = 0. κ_{conn} values: `final_multiplicity` = 0.750; all other encodings = 0.010.

B.5 Phase 3B: STRUC-I summary

Encoding	State	$\langle A_\kappa \rangle$	$\min A_\kappa$
route_transition_code	GP/BS	0.9851	0.9765
closure_transition_code	GP/BS	0.9839	0.9735
category_transition_code	GP/BS	0.9776	0.9645
transition_class_code	GP/BS	0.9775	0.9675
transition_family_code	GP/WP	0.9673	0.9585
layer_transition_code	GP/WP	0.9537	0.9355
composite_count_delta	SB/TS	0.9098	0.8835
externalization_delta	SB/TS	0.8605	0.8360
final_total_charge	SB/TS	0.8118	0.7695
composite_final_count	SB/TS	0.8086	0.7760
external_final_count	SB/TS	0.8116	0.7720
composite_initial_count	SB/TS	0.6372	0.5835
external_initial_count	SB/TS	0.6351	0.5940

C Layer D Boundary-Absence Objects

The four Layer D objects are reproduced below for reference. These are the structural boundary conditions of the charge-routing system.

1. **Free quark (L_D_001).** PDG section: Quarks / Free Quark Searches. Status: not confirmed. Closure class: `TERMINAL_FREE_FRACTIONAL`. Route class: `BOUNDARY_ABSENCE`. Source: PDG RPP 2026 Quarks summary ("all free-quark searches since 1977 have had negative results").
2. **Magnetic monopole (L_D_002).** PDG section: Searches / Magnetic Monopole Searches. Status: not confirmed (best limits from cosmic-ray flux constraints). Closure class: `UNRESOLVED_DUAL_BOUNDARY`. Route class: `DUAL_BOUNDARY_CANDIDATE`. Source: PDG RPP 2026 Searches.
3. **Neutron charge-violating mode (L_D_003).** Candidate mode: $n \to p + \nu_e + \bar{\nu}_e$. Status: constrained by upper bound. Closure class: `CONSTRAINED_CHARGE_VIOLATION_BOUNDARY`. Source: PDG RPP 2026 Baryons.
4. **Proton–electron charge mismatch bound (L_D_004).** Bound: $|q_p + q_e|/e < 10^{-21}$. Closure class: `EXTERNAL_NEUTRALITY_CONSTRAINT`. Route class: `BOUNDARY_CONSTRAINT`. Source: PDG RPP 2026 Baryons.

D Phase 3C Forbidden Boundary Corpus and Chamber Results

D.1 Phase 3C corpus schema

The Phase 3C corpus (`phase3C_forbidden_constrained_transition_corpus.csv`) contains 48 rows and 71 columns. Each row represents one candidate transition, encoding route, closure, category, transition-type, and diagnostic flags. The schema extends the Phase 3B transition encoding with six additional contrast-specific columns: `allowed_vs_forbidden_code`, `boundary_pressure_index`, `boundary_response_code`, `transition_status_code`, `route_charge_consistency_code`, and `closure_charge_consistency_code`.

D.2 Group counts

Group	Type	Count
A	Allowed controls (Phase 3B interior)	12
B	Charge-violating mock transitions	8
C	Free-fractional externalization attempts	8
D	Selection-rule violating comparison channels	8
E	Route-incoherent charge-conserving mocks	8
F	Constrained or upper-bounded boundary cases	4
	Total	48

Charge balance: 40 rows charge-balanced; 8 rows deliberately violate charge balance (Group B).

D.3 STRUC-PERC-I summary

Metric	Value
Ladders submitted	43
Completed results	42
Full Percolation	42
Hard Fragmentation	0
No-result (low-information)	1 (`allowed_control_flag`)

Notable connectivity thresholds: `free_fractional_externalization_flag` $\kappa_{\text{conn}} \approx 0.750$; `boundary_pressure_index` $\kappa_{\text{conn}} \approx 0.562$; all other key encodings $\kappa_{\text{conn}} \approx 0.010$.

D.4 STRUC-I summary

Regime / State	Count	Examples
GP / Boundary-Stabilized	3	closure_trans., category_trans., transition_family
GP / Weak Persistence	5	allowed_vs_forbidden, route/closure_charge_consistency, transition_class, ...
SB / Transitional	33	route_transition, transition_status, boundary_pressure, flags
SB / Near-Critical	2	initial_multiplicity, initial_fractional_external_count
Total	43	

D.5 Phase 3C vs Phase 3B comparison

The decisive contrast: in Phase 3B (38 allowed transitions), `route_transition_code` reaches Geometric Persistence / Boundary-Stabilized with $\langle A_\kappa \rangle = 0.985$. In Phase 3C (48 mixed candidates), `route_transition_code` falls to Structural Boundary / Transitional Structure with $\langle A_\kappa \rangle = 0.859$. `closure_transition_code` remains Geometric Persistence / Boundary-Stabilized in both ($\langle A_\kappa \rangle = 0.998$ in Phase 3C, up from 0.984 in Phase 3B), confirming that the collapse is selective to the route-transition coordinate.

References

[1] Particle Data Group. *Review of Particle Physics*, 2026 Edition. Summary tables used: Leptons, Gauge and Higgs Bosons, Quarks, Mesons, Baryons, and Searches (files: `rpp2026-sum-leptons.pdf`, `rpp2026-sum-gauge-higgs-bosons.pdf`, `rpp2026-sum-quarks.pdf`, `rpp2026-sum-mesons.pdf`, `rpp2026-sum-baryons.pdf`, `rpp2026-sum-searches.pdf`). Available at `https://pdg.lbl.gov`. All Phase 1 corpus assignments and Layer D boundary objects are PDG-sourced or PDG-aligned from these tables.

[2] UNNS Substrate Research Program. *The Margin-Confinement Law: Hard-Boundary Invariance in Universal Ladder Systems*. Working manuscript, 2025.

[3] UNNS Substrate Research Program. *Admissible Cluster Geometry: Recoverable Connectivity in Realizability Space*. Working manuscript, 2026.

[4] UNNS Substrate Research Program. *Admissible Boundary Routing: Structural Classification of Terminal Approach, Finite Bounce, and Cosmological Recession*. Working manuscript, 2026.

[5] UNNS Substrate Research Program. *Stellar Boundary Dynamics I: Boundary Percolation and Bridge Geometry in Core-Collapse Supernova Observational Phases*. Working manuscript, 2026.

[6] UNNS Substrate Research Program. *Phase 3C — Constrained and Forbidden Transition Boundary Tests: Chamber Comparison Report.* Charge Boundary Routing I internal report, 2026. Report file: `PHASE3C_FORBIDDEN_BOUNDARY_chamber_comparison_report.txt`. Corpus: `phase3C_forbidden_constrained_transition_corpus.csv` (48 rows).